

Prediction of Hard Projectile Penetration on Concrete Targets

*Hyeon-Jong Hwang¹⁾, Sanghee Kim²⁾, and Thomas Kang³⁾

¹⁾ *College of Civil Engineering, Hunan University, Hunan 410082, China*

^{2), 3)} *Department of Architecture and Architectural Engineering, Seoul National University, Seoul 151-744, Korea*

¹⁾ hwanggun85@naver.com

ABSTRACT

Various empirical models have been proposed to predict the penetration depth of hard projectiles into concrete targets. Unlike the existing models, the present study focuses on the resistant energy of the concrete target and kinetic energy of the projectile. The resistant energies due to the spalling, tunneling, and scabbing failure of concrete targets under impact load are considered. On the basis of the energy conservation law, the penetration depth of a projectile is estimated.

1. INTRODUCTION

Terrorists' attack and explosion accidents have caused the damage in reinforced concrete structures, which requires the impact resistant design of concrete structures. For this purpose, empirical equations have been proposed to predict the local impact damage of the concrete structures on the basis of the previous test results. Whenever new materials are developed to improve the impact resistance, however, the local impact load resistance of the concrete structures should be evaluated. For civil and military structures, due to the increased terrorists' threat, accurate evaluation of the impact load resistance has become an important issue.

To predict the penetration depth of concrete targets, Petry et al. first considered the impact velocity, projectile mass and sectional area of a projectile, and the concrete penetrability factor depending on the concrete strength and rebar placement (Kennedy 1976). The ACE (1946) evaluated the allowable concrete target thickness that limits perforation and scabbing failure as well as penetration depth, and the NDRC proposed the nose shape effect of projectiles (NDRC 1946; Kennedy 1966). Forrestal et al. (1994) proposed the effect of the concrete density and caliber-radius-head for ogive-nose projectiles. Almusallam et al. (2013) considered the effect of hybrid-fiber reinforced

¹⁾ Assistant Professor

²⁾ Ph.D. Candidate

³⁾ Associate Professor

concrete. Since the existing models for penetration depth were based on the existing test results, the applicability of the existing models is quite limited within the verified test parameters.

The present study focuses on the impact resistant energy of concrete and kinetic energy of a hard projectile. The proposed model should better predict the penetration depth of concrete under impact load.

2. ENERGY BASED MODEL

2.1 Energy Resistance of Concrete Target According to Failure Mode

Fig. 1 shows the impact resistant energy of a concrete target according to failure mode. In the figure, the initial velocity V_i of the projectile develops the kinetic energy E_K , which causes the impact damage in the concrete target. On the basis of the failure mode under impact load, the resistant energy E_R of the concrete target consists of the spalling resistant energy E_S , tunneling resistant energy E_T , and scabbing resistant energy E_C . According to the energy conservation law, the kinetic energy E_K is the same as the resistant energy E_R .

$$E_K = \frac{m}{2}(V_i^2 - V_r^2) \quad (1)$$

$$E_R = E_S + E_T + E_C \quad (2)$$

where m = projectile mass; V_i = initial velocity of the projectile; and V_r = residual velocity of the projectile after perforation.

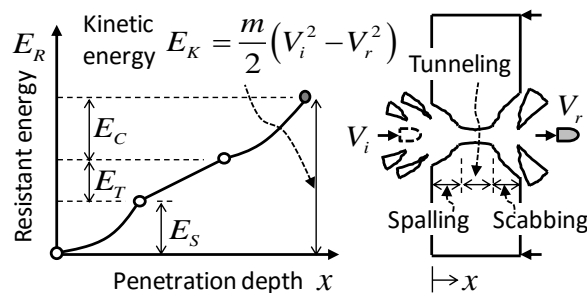


Fig. 1 Impact energy resistance of concrete target

2.2 Spalling Energy E_S

On the projectile collision, the reflected impact force causes the concrete cone failure in spalling region. Fig. 2(a) shows the idealized concrete cone failure. On the concrete cone surface, direct punching shear failure occurs. In the present study, modifying the punching shear model of Choi et al. (2014), the resistance F_S of the concrete cone under impact load is defined.

$$F_s = \left[f_{td} t_s b_s \tan \theta_s + f_{td} \frac{\pi d^2}{4} \right] (k_s k_{bs}) \quad (3)$$

where f_{td} = tensile strength increased by strain rate (fib 2010); t_s = allowable spalling depth ($= k_1 k_2 k_3 k_4 d \leq 0.5h$); k_1 = coefficient related to the concrete target thickness ($= 2.1(h/d)^{0.3} - 1.75 \geq 0$); k_2 = coefficient related to the steel fiber volume ratio V_f ($= 1 - 0.025V_f$, in %); k_3 = coefficient related to the concrete density ρ_c ($= 5.94 - (2.1\rho_c)/1000 \leq 1$, in kg/m^3); k_4 = coefficient related to the maximum size s_a of coarse aggregate ($= 0.23s_a/d + 0.77 \geq 1$); θ_s = average angle of the concrete cone surface; $\tan \theta_s = 2.0$ for flat-, 1.9 for round-, 1.55 for ogive-, and 0.9 for sharp-nose shaped projectile on the basis of the existing test results (Abdel-Kader 2014; Almusallam 2013, 2015; Dancygier 1996, 2007; Kim 2014; Soe 2013; Wu 2015; Zhang 2005); b_s = average perimeter of the concrete cone ($= \pi(d + t_s \tan \theta_s)$); k_s = size effect factor ($= (300/h)^{0.25} \leq 1$, in mm); and k_{bs} = stress concentration effect factor. Note that the contribution of rebars is neglected because the rebar strength in the concrete cone with a low rebar ratio is relatively small.

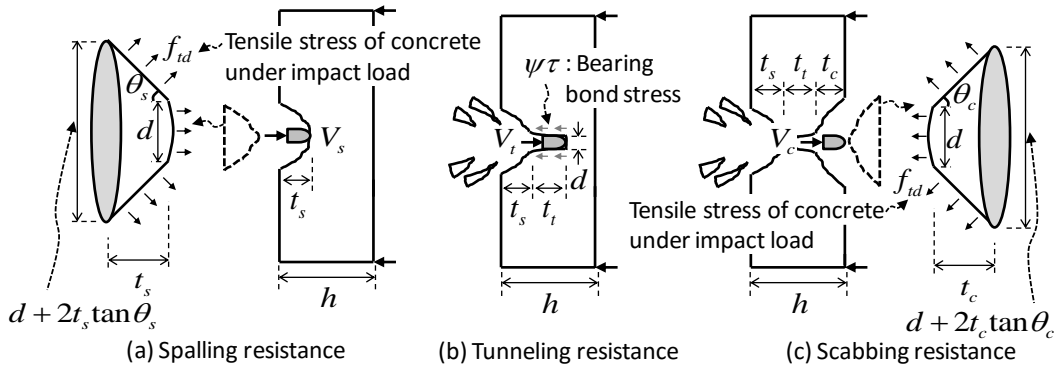


Fig. 2 Failure Mode of Concrete Targets

The Model Code (fib 2010) prescribes the tensile strength f_{td} depending on the strain rate.

$$f_{td} = f_t (10^6 \dot{\epsilon}_c)^{0.018} \quad \text{for} \quad \dot{\epsilon}_c < 10/s \quad (4)$$

$$f_{td} = 0.0062 f_t (10^6 \dot{\epsilon}_c)^{1/3} \quad \text{for} \quad \dot{\epsilon}_c \geq 10/s \quad (5)$$

where f_t = concrete tensile strength, and $\dot{\epsilon}_c$ = strain rate of concrete, which is defined as follows (Kim 2010):

$$\dot{\epsilon}_c = \frac{V_i^2}{h} \sqrt{\frac{\rho_p}{E_p}} \quad (6)$$

where h = concrete target thickness; ρ_p = projectile density; and E_p = elastic modulus of the projectile.

The concrete tensile strength f_t can be determined from the concrete compressive strength according to the Model Code (fib 2010).

$$f_t = 0.3f_c'^{2/3} \quad \text{for} \quad f_c' < 50 \text{ MPa} \quad (7)$$

$$f_t = 2.12 \ln[1 + 0.1(f_c' + 8)] \quad \text{for} \quad f_c' \geq 50 \text{ MPa} \quad (8)$$

The resistance F_S of the concrete cone is increased by the addition of steel fibers. According to Musmar (2013), the tensile strength f_{ts} of steel fiber-reinforced concrete is related to the volume ratio of steel fibers to concrete.

$$f_{ts} = f_t \left(1 + \frac{2}{3} \frac{l_f}{d_f} V_f \right) \quad (9)$$

where f_t = concrete tensile strength without steel fibers; l_f = steel fiber length; d_f = steel fiber diameter; and V_f = volume ratio of steel fibers to concrete. When steel fibers are used, f_{ts} of Eq. (9) is applied to f_t in Eqs. (4) and (5).

In spalling region, assuming an idealized concrete cone failure, the spalling resistant energy E_S is determined as follows:

$$E_S = F_s \frac{V_{sc}}{A_{sp}} = \frac{\pi}{12} f_{td} [4t_s^3 \tan^2 \theta_s + 6dt_s^2 \tan \theta_s + 3d^2 t_s] (k_s k_{bs}) \quad (10)$$

where V_s = velocity of the damaged concrete cone; A_{sp} = projected area of the idealized concrete cone ($= 0.25\pi(d + 2t_s \tan \theta_s)^2$); and V_{sc} = volume of the idealized concrete cone ($= \pi t_s [4t_s^2 \tan^2 \theta_s + 6dt_s \tan \theta_s + 3d^2] / 12$).

2.3 Tunneling Energy E_T

Fig. 2(b) shows the failure mode in tunneling region. In this step, the projectile penetrates the concrete target, and the projectile velocity is decreased by the bond resistance between the projectile and concrete. The bond resistance can be defined as follows:

$$F_t = (\pi dt_t) \psi \tau \quad (11)$$

where t_t = allowable tunneling depth; ψ = nose shape factor of the projectile (= 1.0 for flat, 0.9 for round, 0.7 for ogive, and 0.2 for sharp); and τ = bond stress (= $2.2\sqrt{f'_c}$ by Lowes (2003)).

Applying the strain rate effect of concrete to the bond resistance F_t in Eq. (11), the tunneling resistant energy E_T is determined as follows:

$$E_T = \frac{F_t}{\rho_p A_p} m = \frac{4m}{\rho_p d} t_t (2.2\psi\sqrt{f'_{cd}}) \quad (12)$$

where A_p = cross-sectional area of the projectile, and f'_{cd} = compressive strength depending on the strain rate (fib 2010).

$$f'_{cd} = f'_c (10^5 \dot{\epsilon}_c / 3)^{0.014} \quad \text{for} \quad \dot{\epsilon}_c < 30/s \quad (13)$$

$$f'_{cd} = 0.012f'_c (10^5 \dot{\epsilon}_c / 3)^{1.3} \quad \text{for} \quad \dot{\epsilon}_c \geq 30/s \quad (14)$$

2.4 Scabbing Energy E_C

Fig. 2(c) shows the idealized concrete cone failure in scabbing region. Because the scabbing failure mode is similar to the spalling failure mode, the scabbing resistant energy E_C can be determined by using the same method of the spalling resistant energy E_S .

$$E_C = \frac{\pi}{12} f_{td} [4t_c^3 \tan^2 \theta_c + 6dt_c^2 \tan \theta_c + 3d^2 t_c] (k_s k_{bc}) \quad (15)$$

where t_c = allowable scabbing depth (= t_s); and θ_c = average angle of the concrete cone surface ($\tan \theta_c = 2.0$ regardless of the nose shape of the projectile).

3. PENETRATION DEPTH

In the present study, for simple calculation, the followings are assumed: 1) From $x = 0$ to $h - t_c$, the penetration depth x increases linearly according to the resistant energy; 2) The allowable spalling depth t_s is the same as the allowable scabbing depth t_c ; and 3) On the basis of the test results, the stress concentration effect factors k_{bs} and k_{bc} were fixed as 1.25. In light of the above assumptions, the penetration depth is simplified as a function of the maximum resistant energy $E_R = E_S(t_s) + E_T(h - 2t_s) + E_C(t_s)$ of the concrete target, as shown in Eq. (16). This equation applies only when the kinetic energy $E_K = mV_i^2/2$ of the projectile is less than the maximum resistant energy E_R of the concrete target, which is defined depending on the nose shape (see Eqs. (17) to (20)).

$$x = \frac{mV_i^2}{2E_R}(h - t_s) \quad (16)$$

For flat nose,

$$E_R = \pi f_{td} [2.7t_s^3 + 2dt_s^2 + 0.5d^2t_s](1.25k_s) + 8.8m\sqrt{f'_{cd}}(h - 2t_s)/\rho_p d \quad (17)$$

For round nose,

$$E_R = \pi f_{td} [2.5t_s^3 + 1.9dt_s^2 + 0.5d^2t_s](1.25k_s) + 7.9m\sqrt{f'_{cd}}(h - 2t_s)/\rho_p d \quad (18)$$

For ogive nose,

$$E_R = \pi f_{td} [2.1t_s^3 + 1.8dt_s^2 + 0.5d^2t_s](1.25k_s) + 6.2m\sqrt{f'_{cd}}(h - 2t_s)/\rho_p d \quad (19)$$

For sharp nose,

$$E_R = \pi f_{td} [1.6t_s^3 + 1.4dt_s^2 + 0.5d^2t_s](1.25k_s) + 1.8m\sqrt{f'_{cd}}(h - 2t_s)/\rho_p d \quad (20)$$

4. CONCLUSIONS

In concrete structures, underestimation of impact penetration depth may increase the vulnerability to impact. In the present study, an energy-based model was developed to more accurately predict the penetration depth of a projectile in a concrete target. Itemized impact resistant energy of the concrete target was proposed on the basis of the three failure modes: spalling, tunneling, and scabbing. By comparing the maximum impact resistant energy of the concrete target and kinetic energy of the projectile, the penetration depth can be better estimated.

ACKNOWLEDGEMENT

This research was financially supported by the Youth Program of Hunan University. The authors are grateful to the authorities for their support.

REFERENCES

- Abdel-Kader, M., and Fouda, A. (2014), "Effect of Reinforcement on the Response of Concrete Panels to Impact of Hard Projectiles," *International Journal of Impact Engineering*, **63**(1), 1-17.
- ACE (1946), "Fundamentals of Protective Structures," *Report AT120 AT1207821*, Army Corps of Engineer, Office of the Chief of Engineers.
- Almusallam, T.H., Siddiqui, N.A., Iqbal, R.A., and Abbas, H. (2013), "Response of Hybrid-Fiber Reinforced Concrete Slabs to Hard Projectile Impact," *International Journal of Impact Engineering*, **58**(1), 17-30.
- Almusallam, T.H., Abadel, A.A., Al-Salloum, Y.A., and Siddiqui, N.A. (2015),

- "Effectiveness of Hybrid-Fibers in Improving the Impact Resistance of RC Slabs," *International Journal of Impact Engineering*, **81**(1), 61-73.
- Choi, K.K., Shin, D.W., and Park, H.G. (2014), "Shear-Strength Model for Slab-Column Connections Subjected to Unbalanced Moment," *ACI Structural Journal*, **111**(3), 491-502.
- Dancygier, A.N., and Yankelevsky, D.Z. (1996), "High Strength Concrete Response to Hard Projectile Impact," *International Journal of Impact Engineering*, **18**(6), 583-599.
- Dancygier, A.N., Yankelevsky, D.Z., and Jaegermann, C. (2007), "Response of High Performance Concrete Plates to Impact of Non-deforming Projectiles," *International Journal of Impact Engineering*, **34**(11), 1768-1779.
- fib (2010), "fib Model Code for Concrete Structures 2010," fib, Ernst & Sohn, Germany, 420.
- Forrestal, M.J., Altman, B.S., Cargile, J.D., and Hanchak, S.J. (1994), "An Empirical Equation for Penetration Depth of Ogive-Nose Projectiles into Concrete Targets," *International Journal of Impact Engineering*, **15**(4), 395-405.
- Kennedy R.P. (1966), "Effects of an aircraft crash into a concrete reactor containment building,," *Anaheim, CA: Holmes & Narver Inc.*
- Kennedy, R.P. (1976), "A Review of Procedures for the Analysis and Design of Concrete Structures to Resist Missile Impact Effects," *Nuclear Engineering and Design*, **37**, 183-203.
- Kim, D.J., Sirijaroonchai, K., El-Tawil, S., and Naaman, A.E. (2010), "Numerical Simulation of the Split Hopkinson Pressure Bar Test Technique for Concrete under Compression," *International Journal of Impact Engineering*, **37**(1), 141-149.
- Kim, S.H., Kang, T.H.K., Hong, S.G., Kim, G.Y., and Yun, H.D. (2014), "Impact Resistance of Steel Fiber-Reinforced Concrete Panels Under High Velocity Impact-Load (in Korean)," *Journal of the Korea Concrete Institute*, **26**(6), 731-739.
- Lowes, L. N. and Altoontash, A. (2003), "Modeling Reinforced-Concrete Beam-Column Joints Subjected to Cyclic Loading," *Journal of Structural Engineering*, **129**(12), 1686-1697.
- Musmar, M. (2013), "Tensile Strength of Steel Fiber Reinforced Concrete," *Contemporary Engineering Sciences*, **6**(5), pp.225-237.
- NDRC (1946), "Effects of Impact and Explosion," *Summary Technical Report of Division 2, V.1*, National Defence Research Committee, Washington, DC, 1946.
- Soe, K.T., Zhang, Y.X., and Zhang, L.C. (2013), "Impact Resistance of Hybrid-Fiber Engineered Cementitious Composite Panels," *International Journal of Impact Engineering*, **104**(1), 320-330.
- Wu, H., Fang, Q., Peng, Y., Gong, Z.M., and Kong, X.Z. (2015), "Hard Projectile Perforation on the Monolithic and Segmented RC Panels with A Rear Steel Liner," *International Journal of Impact Engineering*, **76**(1), 232-250.
- Zhang, M.H., Shim, V.P.W., Lu, G., and Chew, C.W. (2005), "Resistance of High-Strength Concrete to Projectile Impact," *International Journal of Impact Engineering*, **31**(7), 825-841.